

Hepatotoxicity of titanium ion generated from metal implant corrosion

Wenqi Du¹, Wanmin Ni², Jin Chen³

¹School of Medical Technology and Information Engineering, Zhejiang Chinese Medical University, Hangzhou, China

²School of International Business, School of Innovation and Entrepreneurship, Zhejiang International Studies University, Hangzhou, China

³School of Medical Technology and Information Engineering, Zhejiang Chinese Medical University, Hangzhou, China

³Corresponding author

E-mail: ¹1223431446@qq.com, ²niwanmin@zisu.edu.cn, ³chenjin0425@zcmu.edu.cn

Abstract

Titanium ions generated from metal implant corrosion has fueled concern during the routine use of orthopedic implants. Systemic distribution of metal ions has been evidenced by elevated serum metal ion levels in patients with Ti spinal implants. In order to evaluate the biological effects of Ti elevation on the secondly exposed cells, hepatocellular carcinoma cell line HepG2 was used to uncover cytotoxicity of Ti ions and the underlied mechanistic pathways. Exposure to increasing concentration of Ti ions, the cell viability and protein content were decreased, which was partly due to the induction of ROS and apoptosis. In addition, the cell stress responsive pathways MAPK and NF- κ B were significantly activated in a dose- and time-dependent manner, which inspired the reaction of inflammation. However, the activation of MAPK and NF- κ B was not regulated by ROS. The present results demonstrated that low Ti concentrations were capable to induce subtle cellular perturbation after a single cell treatment, supporting the evidence that both inflammatory MAPK/NF- κ B pathways and apoptotic mechanisms may mediated the cytotoxicity of Ti ions.

Keywords: Ti ions, ROS, apoptosis, MAPK/NF- κ B pathways, cytotoxicity

1. Introduction

A dramatic routine use of orthopedic implants has fueled concern regarding metal ion generation due to corrosion, fatigue failure of structural components and wearing of joint replacements [1]. Titanium-based alloys are the most widely used orthopedic materials due to their excellent corrosion resistance resulting from the formation of very stable and protective oxide films on the metallic surface [2]. However, failures of these materials have been observed in the presence of corrosive medium, such as a saline environment, which gives rise to metallic release initially localizing in the first few microns of the surrounding bone. Significant differences were found for Ti⁴⁷ in gingival epithelial cells of patients with dental implant compared with healthy adults [3]. The measured Ti levels were reportedly up to 21 mg/L in fibrous membranes encapsulating implants [4]. Metallic contamination does not stop there. Systemic distribution of metal debris has also been demonstrated by measuring elevated serum metal ion levels in patients with Ti spinal implants, which showed higher Ti concentrations of 2.6 μ g/L than the controls of 0.71 μ g/L [5].

Ti may further be transferred by albumin and transferrin proteins to become lodged in distant organs like livers [6, 7]. Therefore, biological effects of Ti elevation on the secondly exposed cells need to be clarified, helping to unravel the potential for local and systemic complications arising from trace metal releasing in the periimplant environment.

Biocompatibility of Ti and its alloys in biomedical devices has been evaluated. The results revealed that byproducts of Ti implants corrosion elicited high cytotoxicity in human enterocytes HT29 and murine osteoblasts MC3T3, and the safe ion concentrations of 15.5 $\mu\text{g/L}$ for Ti has been established [8-10]. Ti ions influenced mineralization and bone formation by enhancing the expression of receptor activator of NF- κB ligand (RANKL) and osteoprotegerin (OPG) in MC3T3-E1 at 9 $\mu\text{g/L}$, while not in GE-1 [10, 11]. Ti ions also involved in inflammation by enhancing mRNA expression of toll-like receptors-4 (TLR-4), intercellular adhesion molecule-1 (ICAM-1) and activating NF- κB in GE-1 cells, suggesting that Ti ions are in part responsible for monocyte infiltration in the oral cavity by elevating the sensitivity of gingival epithelial cells to microorganisms [12, 13]. In return, inflammation caused Ti passive layer on Ti implants to break down, thereby liberating Ti ions even in the absence of fretting *in vivo* [14]. However, the early molecular signal events underlying osteolysis and cutaneous allergic reactions remains unknown. Moreover, the degree to which the released ionic metals are responsible for cellular stress responses remains unresolved.

In present study, using hepatocellular carcinoma cell line HepG2, dose-dependent cytotoxicity of Ti ion was evaluated by WST-1 assay and apoptosis assay. The early cell stress regulating signals were monitored via ROS production and redox sensitive MAPK/NF- κB signaling pathways activation, helping to evaluate adverse biological effects upon second exposure of Ti during their biomedical application.

2. Materials and Methods

Reagents

Ti ion solutions were prepared from standards for atomic absorption spectrometry (Shijiaoke Biotechnology, Beijing, China) and diluted with cell culture medium under pH monitoring. Primary antibodies used in this study were anti-ERK1/2, phospho-ERK1/2 (Thr202/Thr204), cleaved PARP (Santa Cruz Biotechnology, Santa Cruz, CA, USA); anti-p38, phospho-p38 (Thr180/Tyr182), JNK, phospho-JNK (Thr183/Tyr185) (Epitomics, Burlingame, CA, USA); anti- α -tubulin, GAPDH (HuaAn Biotechnology, Hangzhou, China). Anti-I $\kappa\text{B}\alpha$ antibody was prepared in our laboratory according to standard methods [15]. Rabbit monoclonal phospho-I $\kappa\text{B}\alpha$ (Ser32) antibody was obtained from Cell Signaling Technology (Danvers, MA, USA). Anti-rabbit and anti-mouse secondary antibodies were purchased from Promega (Shanghai, China). N-acetyl-L-cysteine (NAC) was purchased from Beyotime Institute of Biotechnology (Shanghai, China). All other chemicals and reagents were from Sigma (Shanghai, China).

Cell culture

Hepatocellular carcinoma HepG2 cell line was obtained from the Cell Bank of the Chinese Academy of Science (Shanghai, China) and grown at 37 °C in a humidified atmosphere containing 5% CO₂. Medium used for HepG2 culture was Dulbecco's Modified Eagle Medium (DMEM; Gibco, Shanghai, China) supplemented with 10% fetal bovine serum (FBS) (v/v) (Gibco, Shanghai, China), penicillin-streptomycin (20 U/mL and 20 $\mu\text{g/mL}$, respectively) (Invitrogen, Shanghai, China). Cell number was counted by a hemocytometer. Cells at about 80% confluence were split 3 times per week to ensure health and growth as well as the cell performing assays.

Cell viability assay

Cytotoxicity induced by Ti ions was assessed by the MTT tetrazolium assay according to the protocol (Beyotime, Haimen, China). 100 μ L cell solution was distributed into 96-well plates (Corning, Shanghai, China) at a density of 5×10^4 cells/mL. Cells were allowed to settle for 20 h prior to Ti ions (0, 0.6, 6, 12, 24, 48, 96 μ g/mL final concentration in wells) addition for 24 h of continuous exposure. Following exposure to Ti ions, 10 μ L MTT (5 mg/mL) was added to medium for an additional 4 h. Formed formazan was dissolved in 100 μ L formazan solution. The absorbance of each well was measured at 570 nm using a microplate reader 680 (Bio-Rad, CA, USA). Measurement was done in triplicates and data (means \pm SD) were normalized to percentage relative to controls.

Protein content analysis

HepG2 cells were settled in 12-well plates (Corning, Shanghai, China) and exposed to 48 and 96 μ g/mL Ti^{4+} for 1-24 h. After treatment, cells were lysed in 50 μ L lysis buffer (50 mM Tris-HCl, pH 7.4, 150 mM NaCl, 0.5% NP-40, 10% glycerol, 1 mM DTT, 1 mM PMSF, 1 mM NaF and 25 mM glycerophosphate), and the supernatant was collected after centrifugation at $14,000 \times g$ for 10 min at 4 $^{\circ}$ C as the whole cell extract. Protein concentration was measured by a Bradford kit (Sangon, Shanghai, China). Three replicates were set for each treatment and mean \pm SD are presented as percentage relative to the controls.

Annexin V-FITC/PI staining

Cell apoptosis was detected according to the annexin V-FITC/PI staining kit (Invitrogen, Shanghai, China). Briefly, HepG2 cells were pretreated with 48 μ g/mL Ti ions for 6, 12, 24 h. After treatment, the cells were collected and washed twice in cold PBS and suspended in 300 μ L of binding buffer at 2×10^5 cells/mL. The samples were incubated with 5 μ L of Annexin V-FITC and 5 μ L propidium iodide in the dark for 15 min at room temperature. Finally, the samples were analyzed by flow cytometry and evaluated based on the percentage of cells for Annexin V positive.

Fluorescence assay of ROS production

Intracellular ROS (reactive oxidative species) were measured with 2', 7'-dichlorofluorescein diacetate (DCFH-DA, Beyotime, China). DCFH-DA passively diffuses into cells and is deacetylated by esterases to form nonfluorescent 2', 7'-dichlorofluorescein (DCFH) which in the presence of ROS forms the fluorescent product DCF. HepG2 cells were seeded at a density of 2×10^5 /well in 12-well plates. After seeding, the culture wells were treated with 12-48 μ g/mL Ti ions for 24 h. Then the cells were harvested and incubated with 10 μ M DCFH-DA in serum-free medium for 20 min at 37 $^{\circ}$ C in the dark. The fluorescence was measured at 488 nm for excitation and 530 nm for emission with a fluorescence plate reader.

Western blot

HepG2 cells were exposed to Ti ions at concentrations ranging from 12-48 μ g/mL for 0.5-24 h. After incubation, cells were lysed in a buffer containing 50 mM Tris-HCl (pH7.4), 150 mM NaCl, 0.5% NP-40, 10% glycerol, 1 mM DTT, 1mM PMSF and 10 μ g/mL lepeptin and cytosolic fractions were obtained as supernatant after centrifugation at $14,000g$ for 10 min at 4 $^{\circ}$ C. Protein concentration was measured by using Bradford kit and 10 μ g protein was loaded on a 10% SDS-polyacrylamide gel, separated by electrophoresis, and then electroblotted onto PVDF membranes (Millipore, MA, USA). Membranes were incubated for 2 h with different primary antibodies against ERK1/2, p-ERK1/2, p38, p-p38, JNK, p-JNK, I κ B α , p-I κ B α , PARP (cleaved), α -tubulin, GAPDH and subsequent anti-rabbit and mouse secondary antibodies for 2 h. Band staining was visualized with NBT-BCIP kit (Sangon, Shanghai, China) and relative protein levels (represented as treated/control ratio) were determined by Quantity One software.

To evaluate the effect of ROS on MAPK/NF- κ B pathway activation and apoptosis, HepG2 cells were treated 48 μ g/mL Ti ions for 1 h. NAC (1, 5, 10 μ M) was pretreated for 2 h before Ti ion challenge. p-ERK1/2, p-p38, p-JNK, p-I κ B α were detected by Western blot.

Statistical analysis

Data were expressed as mean \pm SD of the three replicates of each treatment and statistical analysis was performed by SPSS 16.0 software. Significant differences in Ti treatment groups compared to control group were analyzed by one-way ANOVA followed by the least significant difference (LSD) for multiple comparisons. $p < 0.05$ was considered statistically significant.

3. Results

Ionic Ti dose-dependently decreased cell viability of HepG2 cells

As presented in Fig. 1A, Ti⁴⁺ exposure significantly decreased HepG2 cell viability even at a concentration as low as 6 μ g/mL. Protein content assay also confirmed a marked time-dependent reduction of total protein concentration with 48 and 96 μ g/ml Ti⁴⁺ treatment (Fig. 1B).

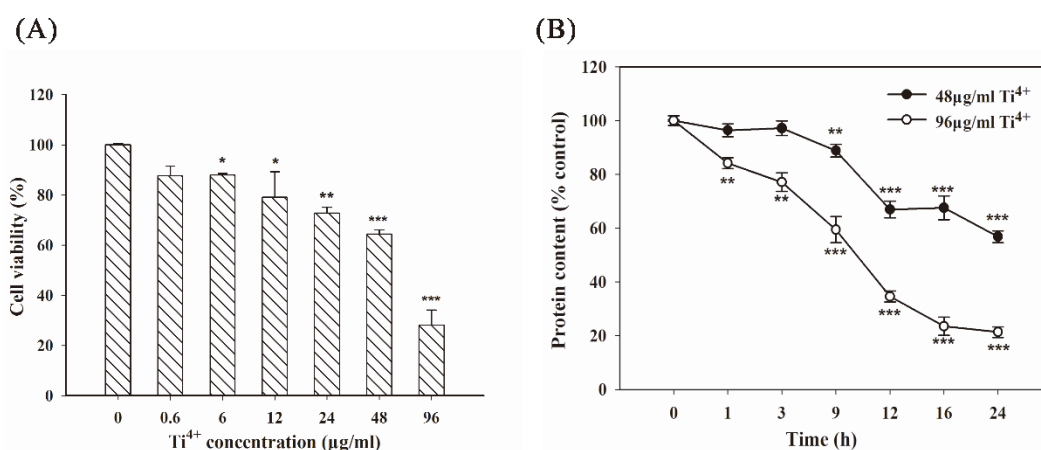


Fig. 1. Cytotoxicity of Ti ion in HepG2 cells. (A) Cell viability of HepG2 cells exposed to Ti⁴⁺ (0.6-96 μ g/mL) for 24 h, evaluated by the MTT assay; (B) Time-dependent effect of Ti⁴⁺ on protein content of HepG2 evaluated by the Bradford assay after exposure to 48 and 96 μ g/mL Ti⁴⁺ for 1-24 h. Data are presented as mean \pm SD (n=3); * $P < 0.05$, ** $P < 0.01$, *** $P < 0.001$ compared with control.

Ti ion triggered apoptosis in HepG2 cells

The apoptosis rate was determined using Annexin V and PI double staining. The release of Ti ion triggered cell apoptosis in a time-dependent manner. The significant apoptosis occurred after 12 h treated with 48 μ g/mL Ti⁴⁺, and the sum of the percentage of both early apoptotic and late apoptotic cells increased to 16.6% after 24 h (Fig. 2A). Meanwhile, cell apoptosis is regulated by caspase-3 activation, which further induces the degradation of PARP [16]. Western blot of cleaved PARP was conducted to evaluate its expression levels after Ti ion stimulation. As shown in Fig. 2B, the expression of cleaved PARP time-dependently increased after 48 μ g/mL Ti⁴⁺ exposure, with the significant change occurring at 2 h earlier than Annexin V/PI assay. The results confirmed the cytotoxicity of Ti ion by triggering cell apoptosis.

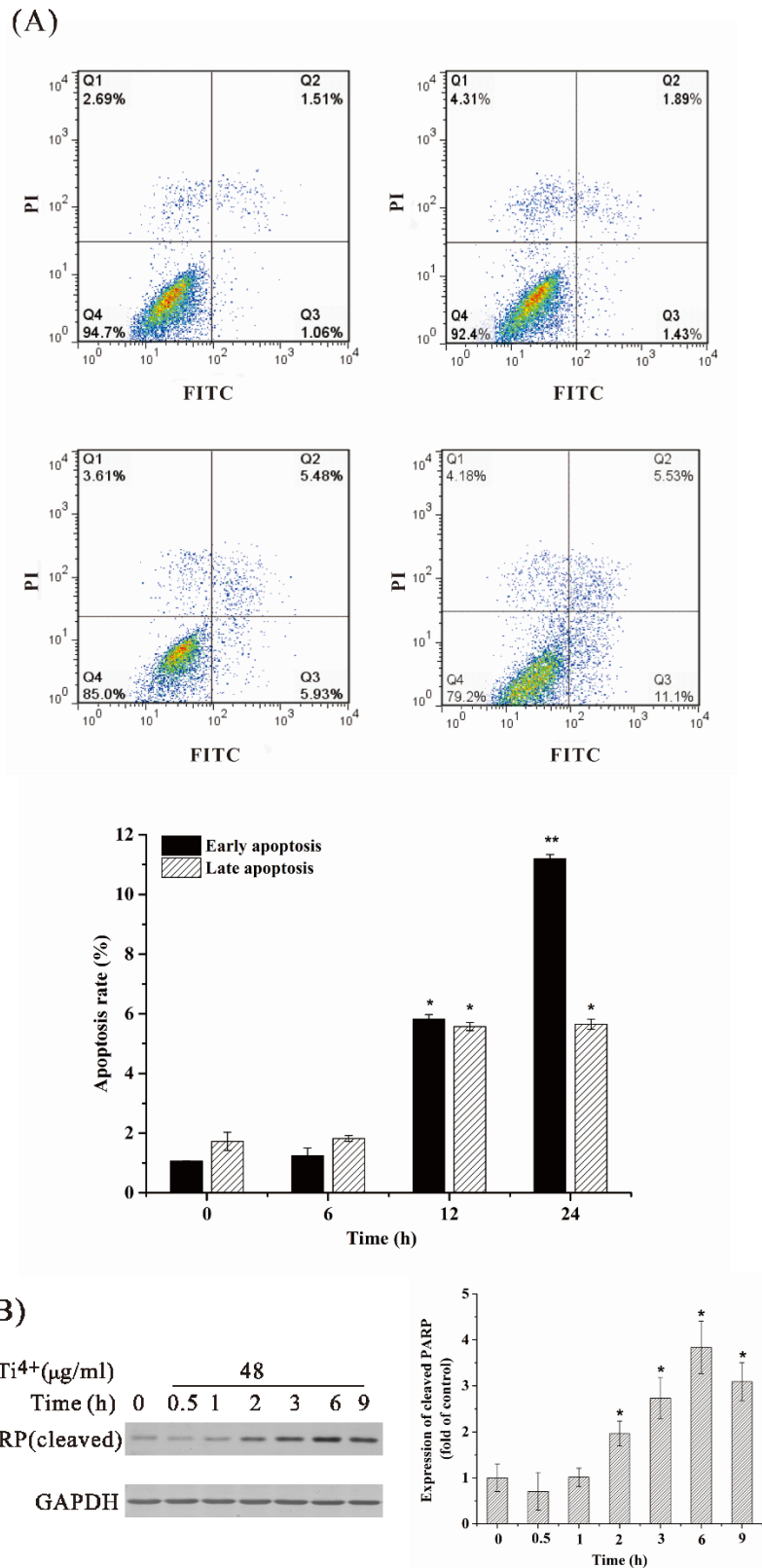


Fig. 2. Apoptosis of HepG2 cells induced by Ti ions. (A) HepG2 cells were exposed to 48 μg/mL Ti⁴⁺ for indicated times. Cells were double stained with FITC Annexin V and Propidium Iodide, and cell apoptosis were determined by flow cytometry assay. (B) Cells were treated with 48 μg/mL Ti⁴⁺ for indicated times. Western blot was performed with PARP (cleaved) antibody and quantified as in the graph. * *P* < 0.05 compared with the control.

Oxidative stress induced by Ti ion

As shown in Fig. 3, Ti ion exposure could significantly induce intracellular ROS production in a time- and concentration-dependent manner. After 12-48 $\mu\text{g/mL}$ Ti^{4+} exposure for 1-12 h, the fluorescence intensity of ROS was increased and sustained in the first 12 h, approximately 6-fold higher than that in the control group, after which the induction level was decreased. However, the ROS was still higher than that in the control, except 48 $\mu\text{g/mL}$ treatment for 12 h.

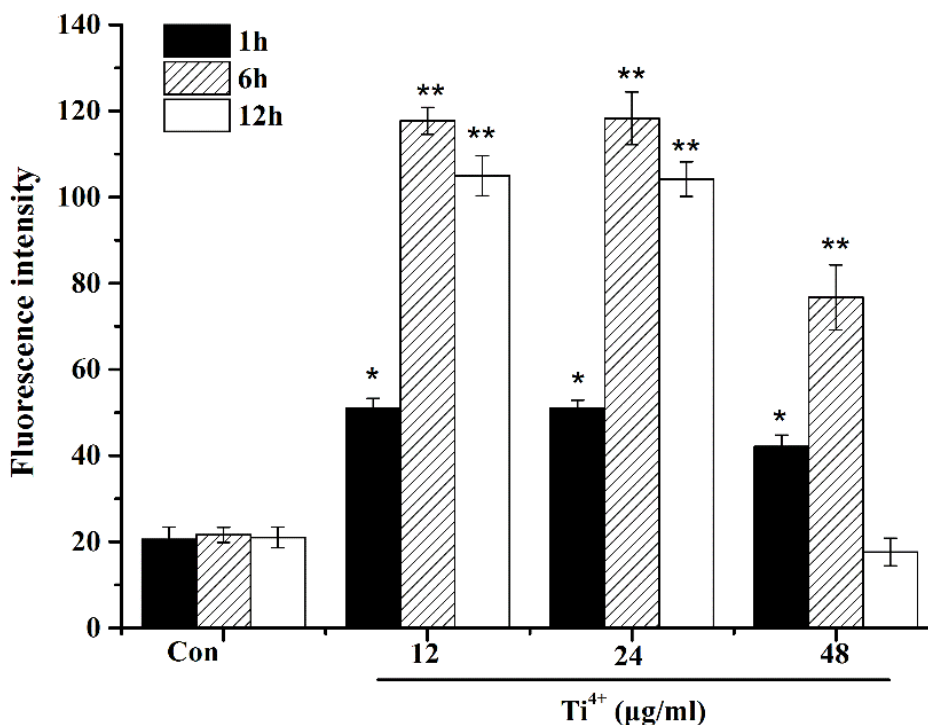


Fig. 3. Ti ion exposure induced ROS generation in HepG2 cells. Cells were treated with 12-48 $\mu\text{g/mL}$ Ti^{4+} for 1, 6, 12 h. Intracellular ROS generation was assessed by DCFDA probe in cells. The data are presented as mean \pm SD, * $P < 0.05$ or ** $P < 0.01$ compared with control.

Dynamic activation of MAPK and NF- κB pathways

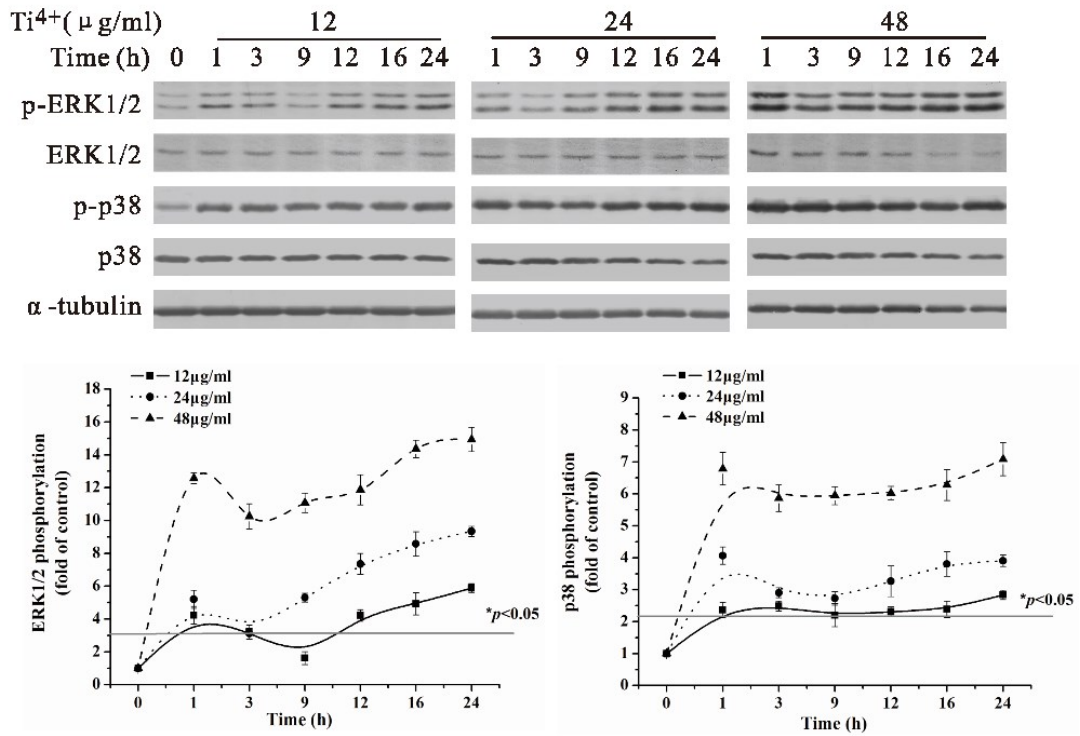
Ti^{4+} exposure yielded significant activation of p38 and ERK1/2 pathways, showing a peak phosphorylation of p38 and ERK1/2 at 1 h followed by a decrease to 9 h and then a progressive enhancement to 24 h (Fig. 4A). A peak phosphorylation of ERK1/2 changed more significantly in range compared with the peak phosphorylation of p38, especially 48 $\mu\text{g/ml}$ Ti^{4+} group. In addition, there were also similar changes in $\text{I}\kappa\text{B}\alpha$ and JNK, showing that peak phosphorylation enhanced to 1 h and subsequently lessened to 9 h under 48 $\mu\text{g/ml}$ Ti^{4+} (Fig. 4B). However, $\text{I}\kappa\text{B}\alpha$ and JNK were less sensitive than p38 and ERK1/2 with no significant phosphorylation under 12 and 24 $\mu\text{g/ml}$ Ti^{4+} exposure (data not shown). These phenomena showed that MAPK and NF- κB pathways were most activated in 1 h to inspire the reaction of inflammatory, then weakened to 9 h, despite any concentration and some gradually increase to 24 h.

Effect of ROS induction on MAPK/NF- κB pathway activation

As cell stress responsive signaling pathways, MAPK and NF- κB pathways could be regulated by oxidative stress [17]. In order to evaluate the effect of Ti^{4+} induced ROS on activation of MAPK and NF- κB pathways, NAC was used to inhibit ROS production. As shown in Fig. 5, Ti^{4+} dramatically induced p38

and ERK1/2 phosphorylation in HepG2, which were not influenced by NAC. Furthermore, Ti^{4+} induced p-I κ B α and p-JNK protein expression could be significantly enhanced by NAC with the growing NAC concentration. The results indicated that Ti^{4+} activated MAPK and NF- κ B pathways independent of its oxidative stress potential.

(A)



(B)

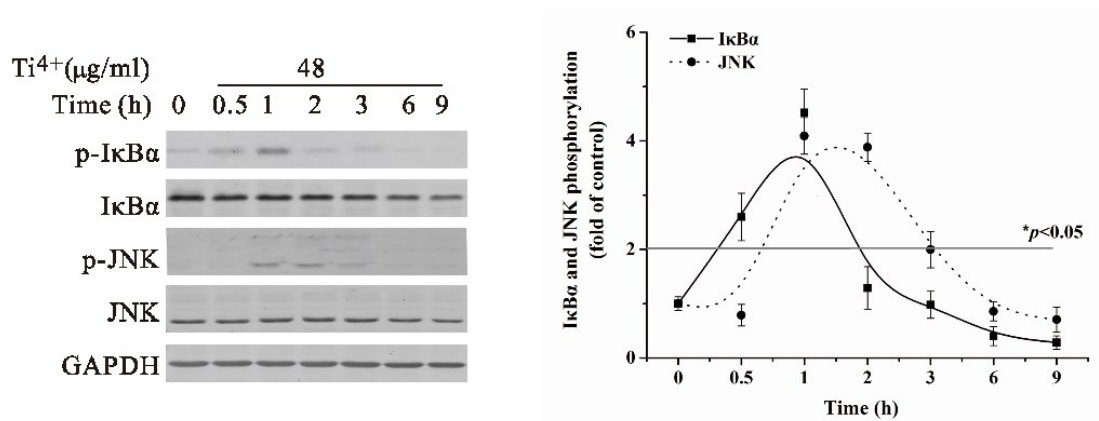


Fig. 4. Ti ion induced activation of MAPK and NF- κ B pathways in HepG2 cells. Cells were treated with 12-48 μ g/mL Ti^{4+} for 1-24 h. Western blot was performed with the indicated antibodies and quantified as in the graph. * $P < 0.05$ compared with the control.

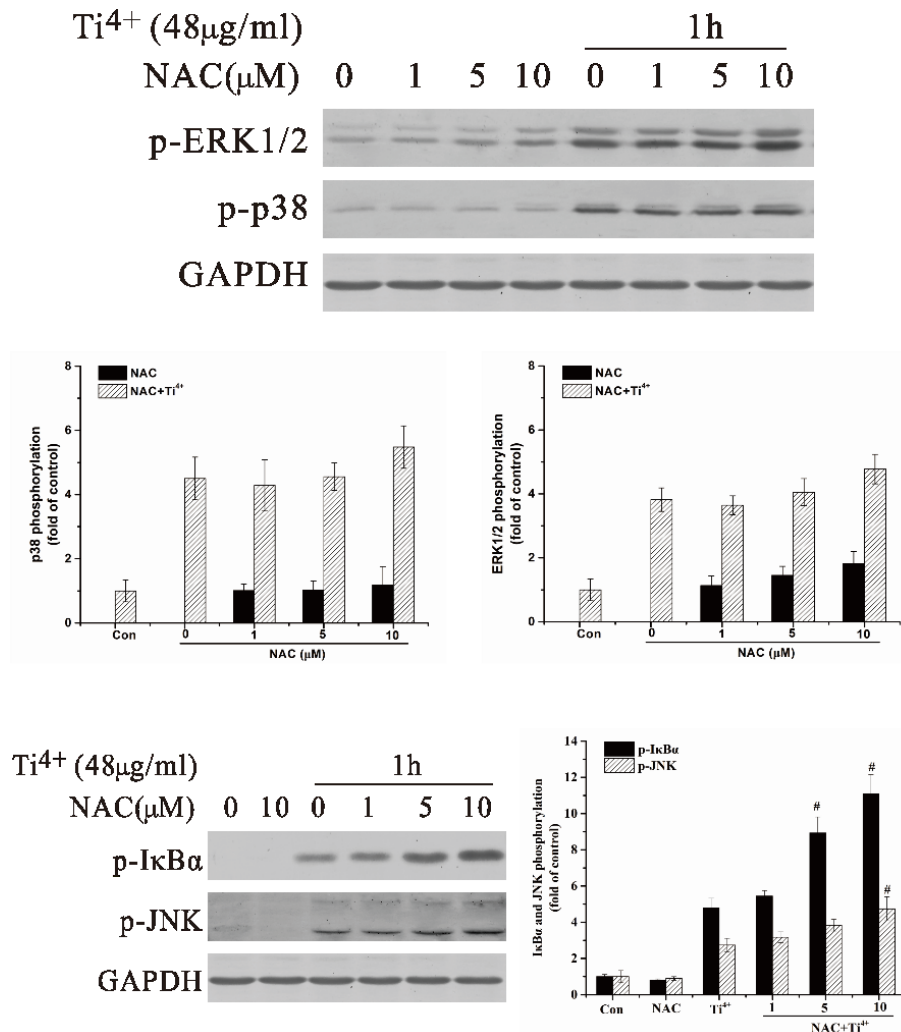


Fig. 5. Effect of ROS on activation of MAPK/NF-κB pathways. HepG2 cells were incubated with Ti⁴⁺ (48 μg/mL) for 1 h with or without 2 h pretreatment with NAC (1, 5, 10 μM). Protein expression was determined by Western blotting with indicated antibodies and quantified as in the graph. # *P*<0.05 compared with Ti⁴⁺ treated group.

4. Discussion

The present study was designed to investigate whether single short-term exposure to Ti ions were able to influence cell fate and understand the molecular mechanism/pathways implicated in cell toxicity. The results showed that Ti ions induced second cytotoxicity to human body when it happened corrosion, fatigue failure of structural components and wearing of joint replacements. With the time extended, more and more ionic Ti were released, which caused the inflammatory reaction of cell to decrease cell viability and protein content in different degree. Ti ions triggered apoptosis with increasingly activating caspase-3, which induced the degradation of PARP. However, it was reported that Ti ions induced cytotoxicity in gingival epithelial-like cells attributed to necrosis, which suggesting that toxicity of Ti ions exerts cell specificity [12].

In order to identify the early signal events underlying inflammation-derived pathogenic effects initiated by Ti ions, we explored dose- and time-dependent activation of the main inflammatory MAPK and NF-κB signaling pathways, which are considered as a first-tier biomarker due to their sensitive inducibility and

regulatory role in cell stress response and inflammation [18]. Ti ions significantly activated ERK1/2, p38 at low concentration of 12 and 24 $\mu\text{g/mL}$ rather than NF- κB and JNK pathway, supporting a paradigm where cellular adaptive responses were triggered counteracting xenobiotics. Moreover, in time course assay, MAPK and NF- κB pathways were generally activated at 1 h and then weakened or stabilized with time elapsing. The time-dependent activation of NF- κB and JNK pathway in a bell curve-like pattern did not exactly follow that of ERK1/2 and p38, which exhibited a progressive enhancement to 24 h, although p38 MAPK is reportedly involved in NF- κB activation by reducing I $\kappa\text{B}\alpha$ levels and inducing NF- κB -DNA binding activity [19]. *In vivo* study also showed that the total amounts of activated NF- κB was highest in Ti exudates after 12 h [13]. The specific signal transduction provides molecular mechanisms to differentiate the distinct cytotoxic potential of Ti ions, making them promising in surveying and managing the risk of Ti ion exposure.

ROS play a dual role in the fate of cell, causing cell death as well as acting as second messengers to induce an adaptive cell response [20]. A hierarchical model for nanoparticle toxicity also described the possibility of higher oxidative stress levels leading to MAPK/NF- κB signal transduction [21], whereas in our study, ROS induced by Ti ions didn't mediate MAPK/NF- κB pathways activation.

5. Conclusion

The present study demonstrated that the Ti ions exhibited different cytotoxicity with varied effective concentration and exposure time, which could partly due to the induction of ROS and apoptosis. Furthermore, inflammatory signaling pathways MAPK and NF- κB were activated at 1 h and could be used as an early warning signal of Ti ions toxicity. These results suggested that Ti ions might decrease cell viability and affect inflammation for local and systemic complications arising from trace metal releasing in the periimplant environment.

References

- [1] Q. Chen, G. A. Thouas. "Metallic Implant Biomaterials." *Materials Science and Engineering R* 87 (2015): 1-57.
- [2] I. Milošev, M. Metikoš-Huković, H. H. Strehblow. "Passive Film on Orthopaedic TiAlV Alloy Formed in Physiological Solution Investigated by X-ray Photoelectron Spectroscopy." *Biomaterials* 21 (2000): 2103-2113.
- [3] P. Lopez-Jornet, F. P. Perez, J. L. Calvo-Guirado, I. Ros-Llor, P. Ramirez-Fernandez. "Metallic Ion Content and Damage to the DNA in Oral Mucosa Cells Patients Treated Dental Implants." *Journal of Materials Science* 25 (2014): 1819-1824.
- [4] L. D. Dorr, R. Bloebaum, J. Emmanuel, R. Meldrum. "Histologic, Biochemical, and Ion Analysis of Tissue and Fluids Retrieved During Total Hip Arthroplasty." *Clinical Orthopaedics and Related Research* 261 (1990): 82-95.
- [5] T. D. Richardson, S. J. Pineda, K. B. Strenge, T. A. Van Fleet, M. MacGregor, J. C. Milbrandt, J. A. Espinosa, P. Freitag. "Serum Titanium Levels After Instrumented Spinal Arthrodesis." *Spine* 33(7) (2008): 792-796.
- [6] Y. Kasai, R. Iida, A. Uchida. "Metal Concentrations in the Serum and Hair of Patients With Titanium Alloy Spinal Implants." *Spine* 28(12) (2003): 1320-1326.
- [7] J. C. Rubio, M. C. Garcia-Alonso, C. Alonso, M. A. Alobera, C. Clemente, L. Munuera, M. L. Escudero. "Determination of Metallic Traces in Kidneys, Livers, Lungs and Spleens of Rats with Metallic Implants After a Long Implantation Time." *Journal of Materials Science* 19 (2008): 369-375.

- [8] J. Soto-Alvaredo, E. Blanco, J. Bettmer, D. Hevia, R. M. Sainz, C. Lopez Chaves, C. Sanchez, J. Llopis, A. Sanz-Medel, M. Montes-Bayon. "Evaluation of the Biological Effect of Ti Generated Debris from Metal Implants: Ions and Nanoparticles." *Metallomics* 6 (2014): 1702-1708.
- [9] Y. Li, C. Wong, J. Xiong, P. Hodgson, C. Wen. "Cytotoxicity of Titanium and Titanium Alloying Elements." *Journal of Dental Research* 89 (2010): 493-497.
- [10] Y. Mine, S. Makihira, H. Nikawa, H. Murata, R. Hosokawa, A. Hiyama, S. Mimura. "Impact of Titanium Ions on Osteoblast-, Osteoclast- and Gingival Epithelial-like Cells." *Journal of Prosthodontic Research* 54 (2010): 1-6.
- [11] H. Liao, T. Wurtz, J. Li. "Influence of Titanium Ion on Mineral Formation and Properties of Osteoid Nodules in Rat Calvaria Cultures." *Journal of Biomedical Materials Research* 47 (1999): 220-227.
- [12] S. Makihira, Y. Mine, H. Nikawa, T. Shuto, S. Iwata, R. Hosokawa, K. Kamoi, S. Okazaki, Y. Yamaguchi. "Titanium Ion Induces Necrosis and Sensitivity to Lipopolysaccharide in Gingival Epithelial-like Cells." *Toxicology in vitro* 24 (2010) 1905-1910.
- [13] F. Suska, C. Gretzer, M. Esposito, L. Emanuelsson, A. Wennerberg, P. Tengvall, P. Thomsen. "In vivo Cytokine Secretion and NF- κ B Activation Around Titanium and Copper Implants." *Biomaterials* 26 (2005): 519-527.
- [14] Y. Mu, T. Kobayashi, M. Sumita, A. Yamamoto, T. Hanawa. "Metal Ion Release from Titanium with Active Oxygen Species Generated by Rat Macrophages *in vitro*." *Journal of Biomedical Materials Research* 49 (2000): 238-243.
- [15] J. E. Celis. *Cell biology - A laboratory handbook*. 3rd ed., pp. 467-482. Elsevier Academic Press, Boston, 2006.
- [16] K. W. Wang. "Molecular Mechanisms of Hepatic Apoptosis Regulated by Nuclear Factors." *Cellular Signalling* 27(4) (2015): 729-738.
- [17] J. J. Meng, X. Zhang, X. C. Guo, W. Cheng, X. Y. Qi, J. Huang, W. H. Lin. "Briarane-type Diterpenoids Suppress Osteoclastogenesis by Regulation of Nrf2 and MAPK/NF- κ B Signaling Pathway." *Bioorganic Chemistry* 112(2021): 104976
- [18] F. Marano, S. Hussain, F. Rodrigues-Lima, A. Baeza-Squiban, S. Boland. "Nanoparticles: Molecular Targets and Cell Signalling." *Archives of Toxicology* 85 (2010): 733-741.
- [19] B. Baeza-Raja, P. Munoz-Canoves. "p38 MAPK-induced Nuclear Factor-kappa B Activity is Required for Skeletal Muscle Differentiation: Role of Interleukin-6." *Molecular Biology of the Cell* 15 (2004): 2013-2026.
- [20] A. W. Kwak, M. J. Lee, M. Lee, G. Yoon, S. S. Cho, J. Chae, J. H. Shim. "The 3-deoxysappanchalcone Induces ROS-mediated Apoptosis and Cell Cycle Arrest via JNK/p38 MAPKs Signaling Pathway in Human Esophageal Cancer Cells." *Phytomedicine* 86 (2021): 153564.
- [21] B. J. Li, M. Tang. "Research Progress of Nanoparticle Toxicity Signaling Pathway." *Life Sciences* 263(15) (2020): 118542.